Role of Si and Ge as impurities in ZnO

J. L. Lyons, A. Janotti, and C. G. Van de Walle
Materials Department, University of California, Santa Barbara, California 93106-5050, USA
(Received 7 July 2009; revised manuscript received 19 October 2009; published 13 November 2009)

The electronic and structural properties of Si in ZnO are studied using density functional calculations with both the generalized gradient approximation and a hybrid functional. Our calculations show substitutional Si on the Zn site (Si_{Zn}) to be significantly lower in energy than the Si interstitial (Si_i) and Si on an O site (Si_O). Si_{Zn} is predicted to be a shallow donor in ZnO with a formation energy low enough to lead to significant incorporation of Si in the ZnO crystal. Interestingly, we find that Si_{Zn} has a lower formation energy (and therefore higher solubility) under Zn-rich conditions than under O-rich conditions. We also study the properties of Ge in ZnO for comparison, finding behavior similar to the Si impurity, but with an even lower formation energy. Our results suggest Si and Ge as suitable *n*-type dopants in ZnO.

DOI: 10.1103/PhysRevB.80.205113 PACS number(s): 71.55.Gs, 61.72.Bb, 74.62.Dh

I. INTRODUCTION

ZnO is a wide band-gap semiconductor that has great potential for solid-state lighting and electronic device applications. With a band gap of 3.4 eV and an exciton binding energy of 60 meV, ZnO has shown high luminescence efficiency in optically pumped lasers and respectable carrier mobilities in bulk crystals and thin films.[1–4] However, the lack of control over its conductivity, especially the difficulties in achieving *p*-type doping, still prevents the material from being fully exploited in semiconductor devices.[4] As-grown ZnO typically exhibits unintentional *n*-type conductivity which traditionally has been attributed to native point defects, in particular oxygen vacancies and zinc interstitials.[5–7] First-principles calculations carried out by several different groups[8–15] all have shown that oxygen vacancies are *deep donors* that cannot be responsible for *n*-type conductivity under equilibrium conditions, although some disagreement remains about the exact position of the defect levels[12–14] and on the role of vacancies in persistent photoconductivity.[13] The calculations also agree that zinc interstitials are shallow donors, but that due to their high formation energy[8,12,13,15] and low migration barrier[11] they also cannot explain unintentional conductivity, except possibly when complexed with impurities.[16] Instead, recent first-principles calculations indicate that the unintentional *n*-type conductivity can be attributed to impurities that are incorporated during growth or processing.[17,18] Among the possible impurities, our results indicated that hydrogen is a likely candidate, since it acts as a shallow donor and is present in almost all growth and processing environments.[17,18] Besides understanding the causes of unintentional *n*-type conductivity in ZnO, it is also desirable to identify suitable *n*-type dopants which give stable *n*-type conductivity with high electron concentrations. This is particularly important for transparent electrical contact applications.

In addition to hydrogen, the possible donors that have been discussed for ZnO include B, Al, Ga, In, Cl, and F.[19] Recent secondary ion mass spectroscopy (SIMS) measurements by McCluskey and Jokela[20] have identified the presence of additional impurities in high-quality ZnO bulk crystals. These single crystals were grown by two distinct methods: a pressurized melt-growth process by Cermet, Inc.[21] and a chemical vapor transport process by Eagle-Picher.[22] The samples were shown to contain measurable concentrations of donors such as Al, Ga, and B. The Cermet samples showed Al concentrations of 2×10^{17} cm^{-3} and the samples from Eagle-Picher showed B and Ga concentrations of $\sim10^{16}$ cm^{-3}. Interestingly, both Cermet and Eagle-Picher samples contained significant concentrations of Si, 1.0×10^{17} and 1.3×10^{17} cm^{-3}, respectively. These sizeable concentrations of Si raise the issue of the effect of this impurity on the electronic properties of ZnO crystals.

Si has four valence electrons and could in principle either substitute for Zn and act as a double donor (Si_{Zn}^{2+}), or substitute for O and act as a double acceptor (Si_O^{2-}). In addition to occupying substitutional sites, silicon could also occupy interstitial sites (Si_i). To our knowledge, the role of silicon in ZnO and more generally the behavior of double donors/acceptors have not yet been explored in ZnO. It is also not clear whether Si would be a shallow (low ionization energy) or deep (high ionization energy) center. These open questions motivated us to investigate the electronic and structural properties of Si in ZnO using first-principles density-functional calculations. We have calculated formation energies for Si in different atomic configurations (Si_{Zn}, Si_O, and Si_i), and transition levels between all possible charge states. We find that Si preferentially replaces Zn in ZnO, acting as a shallow donor (Si_{Zn}^{2+}). The formation energy of Si_{Zn}^{2+} in *n* type is low enough to explain the observed concentrations found in the ZnO bulk crystals.[20] For comparison, we have also studied the electronic and structural properties of Ge in ZnO. Similar to Si, Ge behaves as a double donor (Ge_{Zn}^{2+}) with low formation energy.

II. METHODS

First-principles calculations based on density-functional theory (DFT) have been successfully applied to the study of the electronic and structural properties of defects in semiconductors.[23] The only major shortcoming is the underestimation of the band gap in calculations performed with the local density approximation (LDA) or the generalized gradient approximation (GGA), which may lead to errors in for-

 ©2009 The American Physical Society

TABLE I. Calculated lattice parameters, band gap, and formation enthalpy of ZnO in zinc-blende and wurtzite structures, as well as formation enthalpies of SiO_2 and GeO_2. Both PBE and HSE results are shown. Experimental values from Refs. 33 and 34 are also listed.

Material	Property	PBE	HSE	Expt.
Zinc-blende ZnO	a (Å)	4.62	4.53	4.46
	E_g (eV)	0.63	3.24	3.30
	ΔH_f (eV)	−2.95	−3.26	
Wurtzite ZnO	a (Å)	3.28	3.23	3.25
	c (Å)	5.28	5.20	5.21
	u	0.38	0.38	0.38
	E_g (eV)	0.73	3.35	3.40
	ΔH_f (eV)	−3.08	−3.66	−3.64
SiO_2 (α quartz)	ΔH_f (eV)	−8.47	−8.66	−9.45
GeO_2 (α quartz)	ΔH_f (eV)	−4.95	−5.54	−6.02

mation energies and transition levels of defects in semiconductors.[12,24] Hybrid functionals, which mix a fraction of Hartree-Fock (HF) exchange with the LDA or GGA exchange and correlation potentials, can correct the band gap and, in principle, allow for a better description of formation energies and transition levels. Here we perform calculations using both the GGA and the hybrid functional methods.[25]

Our calculations are based on the DFT and projector-augmented wave potentials[26,27] as implemented in the VASP code.[28,29] The calculations were performed using both the GGA of Perdew, Burke, and Ernzerhof (PBE) (Ref. 30) and the hybrid functional as proposed by Heyd, Scuseria, and Ernzerhof (HSE).[31] In the HSE approach, the exchange potential is separated into long-range and short-range portions, and the HF exchange is mixed with the PBE exchange only in the short-range portion with a characteristic cutoff length of 10 Å. The long-range portion of the exchange potential is still described by PBE and the electronic correlation is also represented by the corresponding part of the PBE functional. Mixing HF exchange only in the short-range part can be considered to be consistent with screening of the electron-electron interactions at large distances. A proportion of 36% HF exchange with 64% PBE exchange produces an accurate value of the band gap and structural parameters in ZnO.[15] Our calculated values along with experimental results are listed in Table I.

The calculations for the impurities were performed using ZnO in the zinc-blende structure. ZnO naturally occurs in the wurtzite structure, but zinc blende has the computational advantage of higher symmetry and has very similar energy and local structure. We therefore expect our results and conclusions for substitutional impurities to be valid also for wurtzite ZnO. Because of the different shape and volume of interstitial cages, results for interstitial configurations could in principle differ between zinc blende and wurtzite; however, as discussed below, our conclusions will not be affected. The systems with impurities were simulated by introducing one Si or Ge in a large ZnO supercell that is periodically repeated in three-dimensional space. In order to address the effects of finite size of the supercells on the formation energy of charged centers we performed calculations for 64-, 216-, and 512-atoms supercells, and extrapolated the results to the dilute limit. We used a plane-wave basis set of 300 eV, and $2\times2\times2$ sets of special k points.

The likelihood of incorporating an impurity in ZnO is determined by its formation energy. For the incorporation of Si on the Zn site (Si_{Zn}), the formation energy is given by

$$E^f(\mathrm{Si}_{\mathrm{Zn}}^q) = E_{\mathrm{tot}}(\mathrm{Si}_{\mathrm{Zn}}^q) - E_{\mathrm{tot}}(\mathrm{ZnO}) - \mu_{\mathrm{Si}} + \mu_{\mathrm{Zn}} + qE_F, \quad (1)$$

where $E_{\mathrm{tot}}(\mathrm{Si}_{\mathrm{Zn}}^q)$ is the total energy of the supercell containing one Si_{Zn} in charge state q, and $E_{\mathrm{tot}}(\mathrm{ZnO})$ is the total energy of a perfect crystal in the same supercell. The Zn atom that is removed from the crystal is placed in a reservoir of energy μ_{Zn}, referenced to the energy of bulk Zn. The Si atom that is added is taken from a reservoir with energy μ_{Si}, referenced to the energy of bulk Si. Expressions analogous to Eq. (1) can be written for the Si_i and Si_O configurations.

The chemical potential μ_{Zn} in Eq. (1) is not constant, but must satisfy the stability condition of ZnO,

$$\mu_{\mathrm{Zn}} + \mu_{\mathrm{O}} = \Delta H_f(\mathrm{ZnO}), \quad (2)$$

where μ_{O} is the chemical potential of oxygen, referenced to the energy per atom of an isolated O_2 molecule and $\Delta H_f(\mathrm{ZnO})$ is the formation enthalpy of ZnO. The solubility of Si in ZnO is limited by the formation of a secondary phase, namely, SiO_2, which imposes an upper limit on the Si chemical potential μ_{Si},

$$\mu_{\mathrm{Si}} + 2\mu_{\mathrm{O}} \leq \Delta H_f(\mathrm{SiO_2}). \quad (3)$$

Focusing on the upper limit [equal sign in Eq. (3)], in the Zn-rich (O-poor) limit we have $\mu_{\mathrm{Zn}}=0$, $\mu_{\mathrm{O}}=\Delta H_f(\mathrm{ZnO})$, $\mu_{\mathrm{Si}}=\Delta H_f(\mathrm{SiO_2})-2\Delta H_f(\mathrm{ZnO})$, and $-\mu_{\mathrm{Si}}+\mu_{\mathrm{Zn}}=-\Delta H_f(\mathrm{SiO_2})+2\Delta H_f(\mathrm{ZnO})$; the latter combination of chemical potentials is relevant since according to Eq. (1) it governs the formation energy of Si_{Zn}. In the O-rich (Zn-poor) limit we have $\mu_{\mathrm{Zn}}=\Delta H_f(\mathrm{ZnO})$, $\mu_{\mathrm{O}}=0$, $\mu_{\mathrm{Si}}=\Delta H_f(\mathrm{SiO_2})$, and $-\mu_{\mathrm{Si}}+\mu_{\mathrm{Zn}}=-\Delta H_f(\mathrm{SiO_2})+\Delta H_f(\mathrm{ZnO})$. From the above considerations, we note that the formation energy $E^f(\mathrm{Si}_{\mathrm{Zn}}^q)$ is actually lower under Zn-rich than under Zn-poor conditions, by an amount $|\Delta H_f(\mathrm{ZnO})|$ (note that the enthalpy of formation is negative for a stable compound). This may seem counterintuitive, as one may expect that silicon would more easily incorporate on a Zn site under Zn-poor conditions, but it follows directly from the above expressions by taking the limit due to SiO_2 formation into account. Note that choosing μ_{Si} from the equality in Eq. (3) corresponds to taking the upper limit of μ_{Si}, and therefore represents the highest concentration (essentially the solubility limit) of Si in ZnO under equilibrium conditions. Lower values of μ_{Si} would lead to higher formation energies and hence lower concentrations of the Si_{Zn} defect.

The calculated enthalpies of formation of ZnO, as well as the solubility-limiting phases, SiO_2 and GeO_2, are also included in Table I. The calculations for SiO_2 and GeO_2 were performed for the α-quartz structure; the difference between the formation enthalpy for GeO_2 in the α quartz and rutile structures is quite small (0.11 eV).

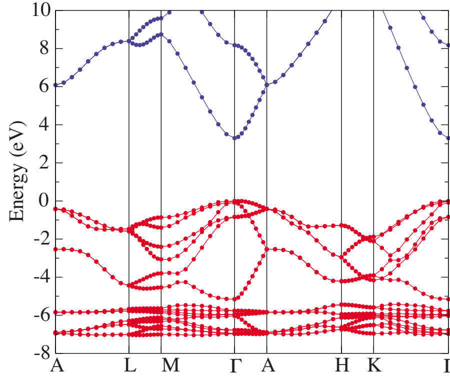

FIG. 1. (Color online) Band structure of wurtzite ZnO calculated using the HSE hybrid functional. The calculated band gap is 3.4 eV and the zero of energy was set at the valence-band maximum.

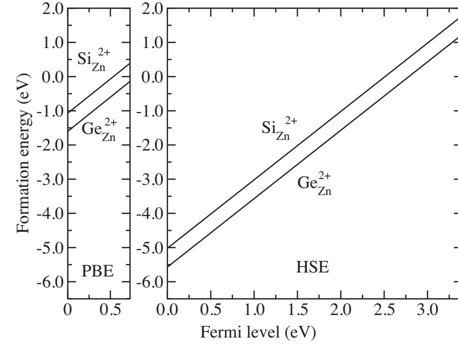

FIG. 2. Formation energies as a function of the Fermi-level position for Si_{Zn} and Ge_{Zn} in ZnO in Zn-rich conditions, according to the (a) GGA-PBE and (b) HSE hybrid functional. In each case the range of Fermi levels corresponds to the computed band gap (0.63 eV in PBE, 3.24 eV in HSE). Both Si_{Zn} and Ge_{Zn} act as shallow donors, with the +2 charge state being stable across the band gap.

III. RESULTS AND DISCUSSION

A. Bulk properties

The calculated lattice parameters, band gaps, and formation enthalpies of ZnO in the PBE and HSE are listed in Table I along with the respective experimental values.[32,33] For comparison we show the results for both wurtzite and zinc-blende ZnO. We can see that PBE slightly overestimates the lattice constants a and c while HSE results are in better agreement with the experimental values. The formation enthalpy of ZnO calculated using HSE is also in closer agreement with the experimental value. As expected, the PBE severely underestimates the band gap (by 76%). This is, in part, due to the underbinding of the Zn d states, which creates too large a repulsion of the bands derived from the O p states that compose the top of the valence band.[34] The HSE corrects this problem, and yields both d-state energies and band gap in much closer agreement with experiment (Fig. 1), in contrast to LDA or GGA results.[34]

B. Energetics and electronic structure

The Si impurity in ZnO can in principle occupy the substitutional sites, Si_{Zn} and Si_O, or the intersititial site, Si_i. Si_{Zn} is expected to act as a double donor (Si_{Zn}^{2+}), whereas Si_O is expected to act as a double acceptor (Si_O^{2-}) in ZnO. Si_i could in principle exist in acceptor and donor charge states. Similar behavior is expected for the Ge impurity, but the atomic size difference between Si and Ge may have effects that can only be assessed by performing explicit calculations.

Our calculations show that Si_{Zn} and Ge_{Zn} are by far the lowest-energy configurations in ZnO. The interstitial configurations Si_i and Ge_i are higher in energy by at least 10 eV across the entire band gap; Si_O and Ge_O are higher in energy by at least 3 eV. We also find that Si_{Zn} and Ge_{Zn} are shallow donors, stable in the +2 charge state (Si_{Zn}^{2+} and Ge_{Zn}^{2+}, respectively) for all positions of the Fermi level in the band gap. Essentially, we find that in both PBE and HSE, the two extra electrons from Si_{Zn} and Ge_{Zn} occupy conduction-band states, which are perturbed by the presence of the impurity. The HSE result is reassuring since it reproduces the experimental value for the ZnO band gap.

The calculated formation energies of Si_{Zn} and Ge_{Zn} in n-type ZnO are relatively low under Zn-rich conditions, as shown in Figs. 2(a) and 2(b) for the PBE and HSE functionals, respectively. This indicates that Si and Ge can be incorporated in ZnO in high concentrations. It is clear from Fig. 2 that it is very difficult to draw conclusions about the nature of the Si_{Zn} and Ge_{Zn} centers in ZnO just based on the GGA-PBE results. The main difference between the PBE and HSE results is due to the fact that the PBE band gap is severely underestimated. We note, however, that the formation energy at $E_F=0$ is much lower in HSE than in PBE. We speculated that this difference might be related to the alignment of the valence-band maximum (VBM) in HSE versus PBE. In order to verify this hypothesis we calculated the band alignment between ZnO in PBE and HSE.

C. Band alignment of ZnO in PBE and HSE

In order to calculate the position of the valence-band maximum (VBM) and conduction-band minimum (CBM) of ZnO in PBE with respect to HSE, we performed separate supercell calculations for a slab geometry of ZnO. In this way the VBM and CBM of ZnO in PBE and HSE are aligned to a common reference (the electrostatic potential at the vacuum region). We used a supercell with 17 atomic layers of ZnO oriented along the nonpolar (110) direction and an equivalent number of layers of vacuum region. The atoms in the three outermost bilayers on each side were allowed to relax. Relaxation has a small effect on the final value of the offset, in this case only 0.1 eV. By comparing the averaged electrostatic potential in the bulk with the vacuum level, and using the position of the VBM and CBM with respect to the averaged electrostatic potential $\bar{V}$, we determined the position of the VBM and CBM with respect to the vacuum level. The results for the PBE/HSE band alignment are shown in Fig. 3.

The hybrid functional corrects the position bands derived from the Zn d states and also partially corrects the effects of self-interaction inherent in the PBE functional. As a result

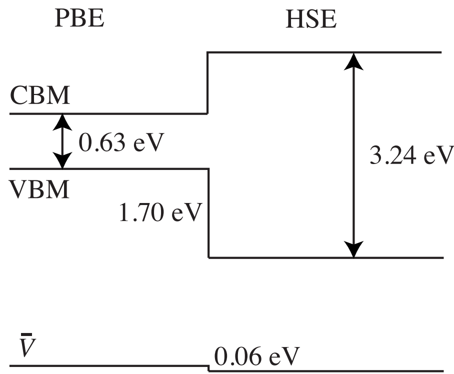

FIG. 3. Alignment between VBM and CBM of zinc-blende ZnO calculated using the PBE and HSE functionals. The alignment of the averaged electrostatic potentials $\bar{V}$ between PBE and HSE is also indicated. The electrostatic potential in vacuum is used as a reference.

the VBM in HSE is about 1.7 eV lower than in PBE as shown in Fig. 3. This difference in the "absolute" position of the VBM accounts for the major part of the difference in formation energies between GGA and HSE values, an effect that has also been noted by Alkauskas and co-workers.[35] E.g., starting from the HSE result for the formation energy of Si_{Zn}^{2+}, at a Fermi-level value of 1.70 eV (corresponding to the position of the VBM in PBE), the value of the formation energy would be $-5.02+2\times1.70=-1.62$ eV. The actual calculated value at the VBM in PBE is -1.07 eV. This remaining difference indicates that the band alignment is not the *only* factor that affects the difference in calculated formation energies.

D. Atomic structure

Figure 4 shows the local lattice relaxation around the Si_{Zn} and Ge_{Zn} impurities. For Si, the nearest neighbor O atoms relax inwards by about 16% of the bond length to give a Si-O bond length of 1.68 Å in HSE (the PBE results differed by only 0.01 Å). This is very close to the calculated Si-O bond length in SiO_2 of 1.61 Å. The Ge defect caused a similar inward relaxation of the nearest neighbors, but to a lesser extent (10%). For both Si and Ge the relaxations are symmetric and no off-site displacements or symmetry breaking

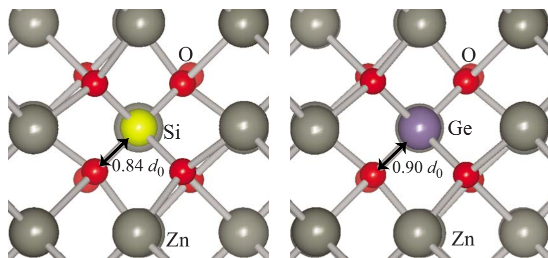

FIG. 4. (Color online) Local lattice relaxations around (a) Si_{Zn}^{2+} and (b) Ge_{Zn}^{2+} centers in the ZnO lattice. Both defects caused an inward relaxation of the nearest-neighbor oxygen atoms. The Si_{Zn}-O and Ge_{Zn}-O bond lengths are indicated expressed as a fraction of the equilibrium Zn-O bond length d_0.

are observed. Possible metastable configurations involving off-site displacements of the impurity or the neighboring atoms in acceptor charge states were also explored. In all cases the displaced atoms were found to relax back to their substitutional positions.

Local lattice relaxation had a strong effect on the electronic properties of the Si and Ge substitutional impurities. Without relaxation, a single-particle Kohn-Sham state induced by Si was found inside the band gap, at 1.60 eV below the CBM in HSE for the +2 charge state (as the Si_{Zn} atom is doubly ionized, this Kohn-Sham state is unoccupied). Allowing lattice relaxations caused the Si-related single-particle state to move upwards above the CBM.

E. Intentional and unintentional doping

The results shown in Fig. 2 refer to the Zn-rich limit conditions, which (as explained in Sec. II) are the most favorable for incorporation of Si and Ge into the Zn lattice site. Strictly speaking, any departure from these conditions would cause the formation energy of Si_{Zn} and Ge_{Zn} to increase. However, the limits imposed by the formation of secondary phases such as SiO_2 and GeO_2 are not rigid, especially in the dilute limit. In any case, the formation energies of Si_{Zn}^{2+} and Ge_{Zn}^{2+} in ZnO under Zn-rich conditions are low enough to allow for the incorporation of these impurities in significant concentrations. Indeed, it has been found by McCluskey and Jokela[20] that Si is present in as-grown single crystals in concentrations of $\sim10^{17}$ cm^{-3}. Since these concentrations are of the same order of magnitude as the carrier concentrations, and since we find Si to act as a shallow donor in ZnO, it is plausible that Si_{Zn} is at least partly responsible for the observed *n*-type conductivity in these samples.

The origin of the Si incorporation in these ZnO single crystals is not known at present. The crystals were grown by two different methods (from the melt and vapor phase transport). We speculate that Si impurities might be present in the Zn sources, since Zn is extracted from minerals from the earth's crust.[36] Alternatively, Si could emanate from some components of the growth equipment, e.g., quartz liners, particularly at the high temperatures required for ZnO crystal growth. The data from Ref. 20 reinforce the notion that rigid control over sources and growth environment is essential for obtaining high purity ZnO substrates and thin films.

The modest formation energies of Si_{Zn}^{2+} and Ge_{Zn}^{2+} lead us to suggest that Si and Ge are good candidates for intentional *n*-type doping in ZnO, since their solubility is expected to be high. This could make them especially suitable for applications in which high carrier concentrations are required, such as for transparent contacts.

IV. CONCLUSIONS

We have investigated the electronic and structural properties of Si and Ge impurities in ZnO based on density functional calculations using GGA (PBE) and hybrid (HSE) functionals. Both Si and Ge were found to favor substitution on the Zn site and act as shallow donors in ZnO, with the +2 charge state being the most stable across the band gap. Si_{Zn}^{2+}

and Ge_{Zn}^{2+} have relatively low formation energies and are more stable under Zn-rich conditions. The calculated formation energy of Si_{Zn} is consistent with the sizeable concentration of Si that is found to be unintentionally incorporated in ZnO crystals.[20] Combined with our finding that Si acts as a shallow donor, our calculations indicate that Si is likely responsible for some fraction of the unintentional *n*-type conductivity in ZnO crystals. Based on our calculations of the electronic properties and formation energies of Si_{Zn} and Ge_{Zn}, we predict that Si and Ge would be suitable donors for *n*-type doping of ZnO.

ACKNOWLEDGMENTS

This work was supported by the NSF MRSEC Program under Grant No. DMR05-20415, by the UCSB Solid State Lighting and Energy Center, and by Saint-Gobain Research. It made use of the CNSI Computing Facility under NSF Grant No. CHE-0321368, and the Ranger supercomputer from the TeraGrid computing resources supported by the NSF under Grant No. DMR070072N. We are grateful to G. Kresse for providing an unreleased version of the VASP code.

[1] D. C. Look, Mater. Sci. Eng., B **80**, 383 (2001).
[2] Ü. Özgür, Y. I. Alivov, C. Liu, A. Teke, M. A. Reshchikov, S. Dogan, V. Avrutin, S.-J. Cho, and H. Morkoç, J. Appl. Phys. **98**, 041301 (2005).
[3] *Zinc Oxide–A material for Micro-and Optoelectronic Applications*, edited by N. H. Nickel and E. Terukov (Springer, Netherlands, 2005).
[4] *Zinc Oxide Bulk, Thin Films, and Nanostructures*, edited by C. Jagadish and S. J. Pearton (Elsevier, New York, 2006).
[5] F. A. Kröger, *The Chemistry of Imperfect Crystals* (North-Holland, Amsterdam, 1974).
[6] K. I. Hagemark, J. Solid State Chem. **16**, 293 (1976).
[7] G. Neumann, in *Current Topics in Materials Science*, edited by E. Kaldis (North Holland, Amsterdam, 1981), Vol. 7, p. 152.
[8] S. B. Zhang, S.-H. Wei, and A. Zunger, Phys. Rev. B **63**, 075205 (2001).
[9] E.-C. Lee, Y.-S. Kim, Y.-G. Jin, and K. J. Chang, Phys. Rev. B **64**, 085120 (2001).
[10] A. Janotti and C. G. Van de Walle, Appl. Phys. Lett. **87**, 122102 (2005).
[11] A. Janotti and C. G. Van de Walle, J. Cryst. Growth **287**, 58 (2006).
[12] A. Janotti and C. G. Van de Walle, Phys. Rev. B **76**, 165202 (2007).
[13] S. Lany and A. Zunger, Phys. Rev. Lett. **98**, 045501 (2007).
[14] T. R. Paudel and W. R. L. Lambrecht, Phys. Rev. B **77**, 205202 (2008).
[15] F. Oba, A. Togo, I. Tanaka, J. Paier, and G. Kresse, Phys. Rev. B **77**, 245202 (2008).
[16] D. C. Look, G. C. Farlow, P. Reunchan, S. Limpijumnong, S. B. Zhang, and K. Nordlund, Phys. Rev. Lett. **95**, 225502 (2005).
[17] C. G. Van de Walle, Phys. Rev. Lett. **85**, 1012 (2000).
[18] A. Janotti and C. G. Van de Walle, Nature Mater. **6**, 44 (2007).
[19] T. Minami, MRS Bull. **25**, 38 (2000).
[20] M. D. McCluskey and S. J. Jokela, Physica B **401-402**, 355 (2007).
[21] D. C. Reynolds, C. W. Litton, D. C. Look, J. E. Hoelscher, B. Claflin, T. C. Collins, J. Nause, and B. Nemeth, J. Appl. Phys. **95**, 4802 (2004).
[22] R. Triboulet, V. Munoz-Sanjosé, R. Tena-Zaera, M. C. Martinez-Tomas, and S. Hassani, in *Zinc Oxide–A Material for Micro- and Optoelectronic Applications* NATO Science Series II Vol. 194, edited by N. H. Nickel and E. Terukov (Springer, Berlin, 2005), pp. 3–14.
[23] P. Hohenberg and W. Kohn, Phys. Rev. **136**, B864 (1964); W. Kohn and L. J. Sham, *ibid.* **140**, A1133 (1965).
[24] P. Rinke, A. Janotti, M. Scheffler, and C. G. Van de Walle, Phys. Rev. Lett. **102**, 026402 (2009).
[25] A. D. Becke, J. Chem. Phys. **98**, 1372 (1993).
[26] P. E. Blöchl, Phys. Rev. B **50**, 17953 (1994).
[27] G. Kresse and D. Joubert, Phys. Rev. B **59**, 1758 (1999).
[28] G. Kresse and J. Furthmüller, Phys. Rev. B **54**, 11169 (1996).
[29] G. Kresse and J. Furthmüller, Comput. Mater. Sci. **6**, 15 (1996).
[30] J. P. Perdew, K. Burke, and M. Ernzerhof, Phys. Rev. Lett. **77**, 3865 (1996).
[31] J. Heyd, G. E. Scuseria, and M. Ernzerhof, J. Chem. Phys. **118**, 8207 (2003).
[32] *Semiconductors—Basic Data*, 2nd ed., edited by O. Madelung (Springer, Berlin, 1996).
[33] A. B. M. A. Ashrafi, A. Ueta, A. Avramescu, H. Kumano, I. Suemune, Y.-W. Ok, and T.-Y. Seong, Appl. Phys. Lett. **76**, 550 (2000).
[34] A. Janotti, D. Segev, and C. G. Van de Walle, Phys. Rev. B **74**, 045202 (2006).
[35] A. Alkauskas, P. Broqvist, and A. Pasquarello, Phys. Rev. Lett. **101**, 046405 (2008).
[36] J. Emsley, *Nature's Building Blocks: An A-Z Guide to the Elements* (Oxford University Press, Oxford, England, 2001), pp. 499–505.